IC/2001/129

United Nations Educational Scientific and Cultural Organization
and
International Atomic Energy Agency

THE ABDUS SALAM INTERNATIONAL CENTRE FOR THEORETICAL PHYSICS

A DETERMINISTIC SEISMIC HAZARD MAP OF INDIA AND ADJACENT AREAS

Imtiyaz A. Parvez
CSIR Centre for Mathematical Modelling and Computer Simulation (C-MMACS), NAL Belur Campus, Bangalore – 560 073, India,
Department of Earth Sciences, University of Trieste, Via E. Weiss 4, 34127 Trieste, Italy
and
The Abdus Salam International Centre for Theoretical Physics, SAND Group, Trieste, Italy,

Franco Vaccari
Department of Earth Sciences, University of Trieste, Via E. Weiss 4, 34127 Trieste, Italy
and
INGV, Institute Nazionale di Geofisica e Vulcanologia, Roma, Italy

and

Giuliano F. Panza
Department of Earth Sciences, University of Trieste, Via E. Weiss 4, 34127 Trieste, Italy
and
The Abdus Salam International Centre for Theoretical Physics, SAND Group, Trieste, Italy.

MIRAMARE – TRIESTE

September 2001

Abstract

A seismic hazard map of the territory of India and adjacent areas has been prepared using a deterministic approach based on the computation of synthetic seismograms complete of all main phases. The input data set consists of structural models, seismogenic zones, focal mechanisms and earthquake catalogue. The synthetic seismograms have been generated by the modal summation technique. The seismic hazard, expressed in terms of maximum displacement (DMAX), maximum velocity (VMAX), and design ground acceleration (DGA), has been extracted from the synthetic signals and mapped on a regular grid of 0.2° x 0.2° over the studied territory. The estimated values of the peak ground acceleration are compared with the observed data available for the Himalayan region and found in good agreement. Many parts of the Himalayan region have the DGA values exceeding 0.6 g. The epicentral areas of the great Assam earthquakes of 1897 and 1950 represent the maximum hazard with DGA values reaching 1.2-1.3 g.

1. Introduction

The Indian subcontinent is one of the most earthquake prone areas of the world. The main seismogenic zones are associated with the collision plate boundary between the Indian and Eurasian plates and are marked by the Kirthar Sulaiman, Himalaya and Arakan-Yoma mountain ranges (Figure 1). Eleven great earthquakes of magnitude 8.0 and above have occurred in this subcontinent during the last two centuries, which clearly indicates the tectonic and structural trends along the collision plate boundary (Figure 2). These devastating earthquakes inflicted heavy casualties and economic damages to the country and the neighbouring areas. One way to mitigate the destructive impact of the earthquakes is to conduct a seismic hazard analysis and take the remedial measures.

The issue of the seismic hazard or the study of destructive effects of earthquakes in India was started by the scientists of the Geological Survey of India (e.g. Oldham, 1899). The first seismic zoning map of India has been compiled by Tondon (1956). It consists of 3 zones based on the broad concept of space-time earthquake statistics and the prevailing understanding of geotectonics. The most severe hazard zones in this map roughly included the Himalayas and the adjoining region in the north, the Chaman fault region in the northwest and the Indo-Burman region in the northeast. The least severe hazard zone covered the Indian shield in the south, with a zone of moderate hazard lying in between. In later years, the Bureau of Indian Standards (BIS) which is the official agency for publishing seismic hazard maps and codes in India, prepared several seismic hazard maps consisting of 6 zones (1962), 7 zones (1966), and 5 zones (1970). The last of these has been reissued in 1984 and it is the current official seismic zoning map of India. According to this zoning, the Peninsular India is considered to be a stable land mass with a region of slight seismicity as it comes in zone I (the region with least hazard). But, the recent Latur (September 30, 1993) and Jabalpur (May 22, 1997) earthquakes show that this zoning needs a critical review and reconsideration.

Various non-official seismic hazard maps for the Indian subcontinent (e.g. Auden, 1959; Mithal and Srivastava, 1959; Guha, 1962; Gaur and Chouhan, 1968; Kaila and Rao, 1979; Khattri *et al.*, 1984; Parvez and Ram, 1997, 1999; Shanker and Sharma, 1998; Bhatia et.al. 1999) have been made available in the literature. Some of

these studies are based on statistical/probabilistic models where the seismic hazard is computed in terms of recurrence in space and time of earthquakes of a given magnitude. Khattri *et al.* (1984) produced a probabilistic seismic hazard map in units of g, for 10% probability of exceedence over the next 50 years period. The most recent study of Bhatia *et al.* (1999) under the Global Seismic Hazard Assessment Program (GSHAP) of IDNDR and ILP is also based on a probabilistic approach. The computational schemes involved in both the studies are: delineation of seismic source zones and their characterizations; selection of an appropriate ground motion attenuation relation with source-site distance and a predictive model of seismic hazard. In the above studies, the attenuation relation produced for the United States (e.g. Algermissen and Perkins, 1976; Joyner and Boore, 1981) has been applied. A comparison of the attenuation relationships for many different areas shows that the attenuation laws may differ very significantly from one region to another due to the differences in the geological characteristics and in the seismic source properties. Recently, Parvez *et al.* (2001) have estimated the attenuation characteristics for the Himalayan region and found a significant difference between the western and eastern parts. Thus, adopting a single attenuation relation from other areas of the world to study the seismic hazard for the Indian region may definitely hamper reliable hazard estimations.

Here, we adopt a deterministic approach in view of the limited seismological data on strong ground motion and of the multiscale seismicity model formulated by Molchan et al., (1997). This model implies that in the probabilistic approach, the seismic zonation must be made at several scales, depending upon the self-similarity conditions of the seismic events and the linearity of the log FM relation, in the magnitude range of interest.

The technique for seismic zoning, developed by Costa *et al.*, (1993), is applied in the present study to prepare a first-order deterministic seismic hazard map for India and the neighbouring areas. This technique has been already used to produce deterministic seismic hazard maps for many areas of the world (e.g. Panza *et al.*, 1996, 1999; Orozova-Stanishkova *et al.*, 1996; Alvarez *et al.*, 1999; Radulian *et al.*, 2000; Aoudia *et al.*, 2000; Zivcic *et al.*, 2000; El-sayed *et al.*, 2001; Markusic *et al.*, 2000; Bus *et al.*, 2000), proving its predicting capabilities wherever new strong earthquakes have occurred, like for instance in Italy for the Umbria-Marche sequence started in 1997.

Realistic synthetic seismograms are constructed by the modal summation technique (Panza, 1985; Panza and Suhadolc, 1987, Florsch *et al.*, 1991; Panza et al., 2001) to model ground motion at the sites of interest, using the available knowledge of the physical process of earthquake generation, level of seismicity and wave propagation in anelastic media. From these synthetic signals engineering parameters can be extracted in order to assess the seismic hazard. Therefore, we can estimate these parameters also in those areas where very limited (or none) historical or instrumental information is available. As examples of the results that can be obtained, we show the maps of the distribution of maximum displacement (Dmax), maximum velocity (Vmax) and design ground acceleration (DGA) over the investigated area.

2. Geology and Tectonics

The general geological and tectonic features of the Indian subcontinent are shown in Figure 1. The entire Indian subcontinent can initially be divided into three main subregions on the basis of general geological and tectonic features (Khattri *et al.*, 1984). The first subregion is formed by the Sulaiman and Kirthar mountain ranges in the north west, the Himalayan Mountains in the north, extending from west to east for a distance of 2500 km, and the Arakan Yoma mountain ranges in the east, extending from north to south into the island arc system of the Andaman Nicobar, Sumatra and Java Islands. The average elevation in this region lies between 1000 to 4500 meters. The second subregion is formed by the vast alluvial plains of the river Sindhu (Indus) and Ganga (Ganges) with an average elevation of about 200 meters. The hills and coastal plains of the Indian Peninsular shield form the third subregion with an average elevation of about 600 meters, although mountain ranges are present within this region having elevations in excess of 2500 meters.

The first subregion is the result of the collision of the Indian and Eurasian plates. The Kirthar Sulaiman ranges consist of numerous Mesozoic and Tertiary arcuate faults and imbricated structures (Krishnan, 1968). The epicentral zones follow the folded belt characterising the area and a major fault system known as Chaman fault, is active along its entire length that runs generally in a NE-SW direction (Verma, 1991). The major tectonic features in the Himalayan mountain ranges include, from south to north, the Main Boundary Thrust (MBT), the Main Central Thrust (MCT) and the Indus-Tsangpo Suture (ITS) all along the entire length of the Himalaya from west to east. The MBT is a series of thrusts that separates the

predominantly pre-Tertiary Lesser Himalayas from the Tertiary Siwalik, composed of fossiliferous Riphean sediments overridden by several thrust sheets (Wadia, 1975; Gansser, 1977). The MCT at the base of the central crystalline zone dips northward separating the High Himalayas from the Lesser Himalayas (Gansser, 1964). The ITS is characterised by the ophiolite suite on the north and demarcates the northern limits of the Indian plate. The Arakan Yoma fold belt consists of a large thickness of Mesozoic and Tertiary rocks intruded by granitic and ultrabasic rocks (Krishnan, 1968). It is a northward continuation into the continent of the Andaman, Nicobar, Sumatra and Java Island arc system and is laced with thrust zones and other faults that have been produced by the collision of the Indian and Burmese plates (Deshikachar, 1974). The fault plane solutions indicate a general northward underthrusting of the Indian Plate in the Himalayan front and an eastward underthrusting in the Arakan Yoma region. The tectonics of the Kirthar-Sulaiman ranges is influenced by transcurrent faulting.

The Sindhu-Ganga Basin (second subregion) is a frontal depression that is filled by the sediments and alluvium. It is also considered the replica of the trench systems, which are associated with the front of island arc systems at subduction zones (Khattri, 1987). It consists of the autochthonous zone in which the Precambrian rocks of the Indian shield are downwarped and plunge under the mountains towards the northwest, north and east forming the foredeep and marginal depression south of the Himalayan tectonic zone. The major subsurface basement faults have been mapped in the area bordering the Himalayan mountains, which reflect the continuation of the tectonic features mapped in Peninsular shield (Eremenko and Negi, 1968; Valdiya, 1973). Infrequent earthquakes clustered in a few localities occur in this subregion.

The third subregion, that is the Peninsular Indian shield, is considered to be a stable landmass and a region of slight seismicity. The detailed geology and tectonic of the region is presented by Valdiya (1973), Naqvi and Rogers (1987) and many others. Geological framework of the region is the cumulative effect of geodynamics sequences ranging from early Precambrian crustal evolution to the young volcanism over its northwest segment. This shield is bounded in the north by the Narmada-Son lineament and Godavari rift system. Major geological entities in the south are Dharwar craton (folding) which is a granite-greenstone terrain, the Eastern Ghat granulite terrain, Deccan volcanic province and the Cuddapah basin.

2. Input data

The computation of realistic synthetic seismograms is highly dependent on our knowledge of the source and propagation effects. Therefore, the input parameters describing the structural models and seismic sources must be properly defined and assigned to the studied area. In general, the input data include four main groups of parameters and these are i) structural models, ii) seismogenic source zones, iii) fault plane solutions, and iv) earthquakes catalogue. The flow chart of the computation process is given by Costa *et al.*, (1993). A brief description of each input parameter for the Indian subcontinent is given below.

2.1 *Structural Model:*

The regional polygons define the structural models separating the areas characterized by different lithospheric properties. The structural models are represented by a number of flat layers, each one described by its thickness, density, P- and S-wave velocities and attenuation. Since the computation is aimed at a first order seismic zonation, the structural models do not explicitly account for local site effects, and are representative of regional average properties (bedrock) within each polygon (Figure 3). In order to propose a suitable structural model, all available geophysical and geological information for the investigated territory have been considered after an extensive bibliographic research (e.g Ram and Mereu, 1977; Roecker, 1982; Lyon-Caen, 1986; Singh, 1987, 1988, 1994; Bourjot and Romanowicz, 1992; Ramesh *et al.*, 1993; Mohan and Rai, 1995; Srinagesh and Rai, 1996; Curtis and Woodhouse, 1997; Mohan *et al.*, 1997; Prakasan and Rai, 1998; Cotte *et. al.*, 1999). As a result, the entire Indian subcontinent has been divided into fifteen regional polygons. The initial boundaries of the polygons are adopted from Mohan *et al.*, (1997) and have been further modified on the basis of the results given in more recent studies (e.g. Curtis and Woodhouse, 1997; Cotte *et al.*, 1999). The structural parameters proposed by different authors for the same polygon have been considered, and an average model has been prepared. While averaging, more weight has been given to the results of the most recent studies. The average structural model of each polygon used in the computations is shown in Figure 4 (a to e), until the depth of 100 km.

Q – structure beneath India has not been very well studied so far. Singh (1991) has estimated the anelasticity of the crust and upper mantle beneath North and Central

India from surface waves analysis. He concluded that the Q-structure beneath North-India reveals the presence of a high attenuating zone at a shallow depth of 20-80 km from the surface and high Q values for the central India from shallow to 100 km. However, a recent study by Parvez *et al.* (2001) on the attenuation of strong motion amplitudes in Himalayan region reveals high Q values for Himalayas for similar depths. This is also in agreement with the Q values (Qp=4000, Qs=2000) used by Yu *et al.* (1995) in their study on the Uttarkashi earthquake of 1991, and with the results obtained by Mitchell *et al.* (1997). Hence, we use high Q values both for the North India as well as the central India.

2.2 *Seismogenic Zones*

Forty seismogenic zones have been defined for the Indian Subcontinent (Figure 5). These zones are classified on the basis of seismicity, tectonics and geodynamics. The seismogenic zones are very dense along the collision plate boundary i.e. along the Kirthar Sulaiman, Hindukush, Himalaya, ArakanYoma and Andaman, whereas one can see gaps between seismogenic zones in Peninsular India. This is because Peninsular India is seismically relatively quiet, and we are interested in earthquakes with magnitude 5 and above and focal depth less than 50 km. We apply the procedure strictly as it has been defined by Costa *et al.*, (1993) in order to produce results consistent with what has already been computed for other countries.

Khattri *et al.* (1984) and Bhatia *et al.* (1999) have defined seismogenic zones for the Indian subcontinent, but we do not consider their zoning as it seems that consistent definition criteria have not been adopted across the entire territory. For example, Khattri *et al.* (1984) divided the whole territory in 25 zones, but some of them are quite big and may not be assumed homogeneous in their properties. Similarly, seismogenic zone no. 1 of Bhatia *et al.* (1999) has not even a single event inside the zone, whereas an earthquake of magnitude 7 lies just outside zone 81. Also, source zones 70 to 75 are based on very small local earthquakes whereas similar size events are not taken into account in the definition of seismogenic zones in other parts of the continent.

2.3 Fault Plane Solutions

Fault plane solutions in the present study are mainly taken from Harvard CMT Catalogues. However, published focal mechanism solutions by Fitch (1970), Molnar

et al. (1973), Chandra (1977; 1978) have been used for the large earthquakes which occurred before 1977 and for the focal mechanism solutions of Peninsular India events. A representative fault plane solution is defined for each seismogenic zone, either looking at the mechanism associated with the strongest event, or with the best obtained event, or the most frequent event. The entire investigated region is dominated by thrust-type and strike slip fault plane solutions, although normal type faulting is present in a few zones (Figure 5).

2.4 Earthquake Catalogue

The earthquake catalogues and databases are the most essential and important parameter for any kind of seismic zoning or hazard studies. In the present paper, the earthquake data set spanning the time interval from 1819 to 1998 has been used. The Indian earthquake catalogue can broadly be divided into three groups: 1) since 1963, based on the WWSSN network and on modern instrumentation; 2) the period 1900-1962, based on the early instrumental data and 3) pre-1900, based on pre-instrumental and historical macroseismic information. Khattri (1987) has reported the completeness of the catalogue threshold as shown in Table 1. With our deterministic approach, catalogue completeness is not as important as in the probabilistic approaches. We are just looking at the spatial distribution of events of magnitude 5 and above, not at their time distribution. We may be underestimating the seismicity only in those seismogenic zones where the occurred strongest event is not reported in the catalogue, but this lack of knowledge would affect also the results of a probabilistic technique. Field studies aimed at the recognition of the seismogenic potential of major active faults are a possible solution to the problem of determining the maximum expected magnitude, as shown by Aoudia *et al.* (2000). The catalogue, which we use, contains Ms, Mb and M_L magnitudes for different time periods. In order to be conservative, if more than one type of magnitude is available for a given event, we use the maximum magnitude. The sources of data are the NOAA earthquake file, Chandra (1978) and the National Earthquake Information Centre of USGS.

3. Computation

In order to obtain a conservative distribution of the maximum observed magnitude over the Indian subcontinent, the seismicity map obtained from the

earthquake catalogue has been smoothed as follows. Initially, the area has been subdivided into a grid of cells of 0.2° x 0.2° (latitude and longitude) and the magnitude of the largest earthquake that occurred within each cell is assigned to it. To partly account for the source dimensions of the largest earthquakes, catalogue incompleteness and localisation errors, the discretised maximum magnitude is smoothed by applying a centred smoothing window (Costa et al., 1993; Panza et al., 1999). After the smoothing of seismicity, only the sources falling within the seismogenic zones are taken into account for the computation of synthetic seismograms. The seismicity map after smoothing is shown in Figure 6. Each source in this figure is a double-couple point source. The strength of the source is determined according to the maximum magnitude assigned to the cell and the orientation of the double-couple point source is the one representative of the parent seismogenic zone. It is assumed that the hypocentral depth is variable, depending on the earthquake magnitude. For sources with $M \leq 7.0$ the hypocentral depth is fixed at 10 km, while for those with $8.0>M>7.0$ it is set equal to 15 km as in previous studies (Panza *et al.*, 1996, 1999; Orozova-Stanishkova *et al.*, 1996; Alvarez *et al.*, 1999; Radulian *et al.*, 2000; Aoudia *et al.*, 2000; Zivcic *et al.*, 2000; El-sayed *et al.*, 2001; Markusic *et al.*, 2000; Bus *et al.*, 2000). For the great events of magnitude larger than 8.0 the hypocentral depth is set to 25 km, and the procedure described in Section 4 has been followed.

The synthetic seismograms have been computed on a grid (0.2° x 0.2°) covering the whole territory under investigation using the modal summation technique (Panza, 1985; Panza and Suhadolc, 1987; Florsch *et al.*, 1991; Panza et al., 2001). In order to avoid the overlapping of sources and receivers, the sources are placed in the centre of each cell falling within the seismogenic zones, whereas the receivers are placed at the grid points (sites) covering the whole investigated area. The synthetic signals are computed for frequencies up to 1 Hz.

At each site, the horizontal components (P-SV radial and SH transverse) synthetic seismograms are first computed for a seismic moment of 10^{-7} Nm and then scaled to the magnitude of the earthquake using the Moment-Magnitude relation of Kanamori (1977). The finiteness of the source is accounted by scaling the spectrum using the spectral scaling law proposed by Gusev (1983) as reported by Aki (1987). For the period between 1 and 2 seconds, the Gusev spectral fall off produces higher

spectral values than the ω^{-2} spectral fall off, and thus guarantees a conservative hazard computation (Vaccari, 1995).

In the case where a source-site path crosses one or more boundaries between structural models, the site structural model is used along the entire path, since the station records are usually more sensitive to the local structural conditions, as shown by Panza et al. (2001) for P-SV waves. The horizontal components at each site are first rotated into a reference system common to the whole territory (N-S and E-W directions) and then the vector sum is calculated. The largest amplitude resulting signal, due to any of the surrounding sources, is selected and associated with that particular site.

Among the representative parameters of the strong ground motion, we focus on the maximum ground acceleration, velocity and displacement (AMAX, VMAX and DMAX). The Fourier spectra of displacements and velocities show that an upper frequency limit of 1 Hz is sufficient to take into account the dominating part of the seismic waves, while this is not true for accelerations (e.g. Panza *et al.*, 1999). On the other hand, the required knowledge about seismic sources and lateral heterogeneities, that might justify the choice of a higher frequency limit in the computations, usually is not available at the scale of the areas generally considered in the zoning.

For acceleration, the deterministic modelling can be extended to frequencies greater than 1 Hz by using the existing standard design response spectra (Panza *et al.*, 1996). The design ground acceleration (DGA) values are obtained by scaling the chosen normalized design response spectrum (normalized elastic acceleration spectra of the ground motion for 5% critical damping) with the response spectrum computed at frequencies below 1 Hz.

4. Computation for Great Earthquakes

In the past 200 years, the Indian subcontinent has experienced eleven great earthquakes of magnitude 8.0 and above inflicting heavy casualties and damages. The events, which occurred in India are Kutch (M=8.3, 1819), Assam (M=8.7, 1897), Kangra (M=8.1, 1905), Bihar-Nepal (M=8.3, 1934) and Assam (M=8.6, 1950). For such great events, the following extension to the method of Costa *et al.* (1993) has been applied. A number of tests have been made to model such great events, keeping in mind the dimensions of rupture, the distribution of magnitude in the surrounding

cells while smoothing, and the source-receiver distances. For the magnitude 8 and above events, epicentral distances up to 300 km have been considered and the smoothing window of radius n=3 cells is used.

5. Scaling for north-east India

Parvez *et al.* (2001) have studied the attenuation of strong motion amplitudes in Himalayas and observed that the peak amplitudes of the eastern Himalayan region are three times larger than those obtained in the western Himalayas and in other parts of the world. Their finding is based on the analysis of six events (Mw=5.2-7.2) recorded by the strong motion arrays installed in western and eastern Himalayas and of the available macroseismic observations. A possible explanation for such anomaly in the ground motion may be found in the high stress drop of the relevant earthquake fault, even if some effects due to Q variations associated with the presence of hydrothermal fluids (Mitchell *et al.*, 1997) cannot be excluded. A similar anomaly is evident in the present study when we compare the synthetic and observed peak amplitudes with our default deterministic modelling. To cope with this problem, we modify the scaling curves (Gusev, 1983) for the eastern Himalayan region. The Gusev (1983) scaling spectra are obtained by a series of averaging procedures and are intended to correspond to the typical global stress drop ($\Delta\sigma$) levels of 30-50 bars. These spectra can be modified to account for other values of the stress drop assuming that, at a given corner frequency (f_c), the (log-) spectral shape is fixed. In such a case, the actual spectrum has the same shape of the typical one but it is multiplied by a coefficient that is proportional to the actual seismic moment and to the deviation of $\Delta\sigma$ from its standard value. If we denote a particular spectrum of Gusev's (1983) family at a given reference seismic moment M_{0ref} as $S_{ref}(f \mid M_{0ref})$, then for another event with $M_0 = M_{0t}$, but with the same corner frequency, we have the spectrum:

$$S_t(f) = (M_{0t}/M_{0ref})\, S_{ref}(f|M_{0ref})$$

or
$$S_t(f) = k(M_0) S_{ref}(f|M_{0ref}) \qquad (1)$$

where $k(M_0) = M_{0t}/M_{0ref}$ is the adjusting coefficient for the whole spectrum.

Now from Brune's model,

$$\Delta\sigma \propto M_0 . f_c^3$$

and $k(\Delta\sigma) \propto k(M_0)$

Hence equation (1) becomes

$$S_t(f) = k(\Delta\sigma) S_{ref}\left(f \middle| M_{0t}/k(\Delta\sigma)\right) \tag{2}$$

Now, our goal is to obtain the coefficient $k(\Delta\sigma)$ for a specific increment in the peak acceleration (e.g. 3 times for the eastern Himalayas).

From Brune's ω^{-2} spectrum, the displacement spectra $SD(f)$ at high frequency is

$$SD(f) \propto \frac{M_0}{1+\left(\frac{f}{f_c}\right)^2} \tag{3}$$

and the acceleration spectra $SA(f)$

$$SA(f) \propto \frac{M_0 f^2}{1+\left(\frac{f}{f_c}\right)^2} \tag{4}$$

for large (f/f_c) i.e. in the high frequency limit, $SA(f)$ reduces to

$$SA(f) \propto M_0 . f^2 = SAHF. \tag{5}$$

From the Parseval's theorem,

$$SA(f)^2_{\max} . 2\Delta f = a^2_{rms} . d \tag{6}$$

where Δf is the effective bandwidth, a_{rms} is the rms acceleration, and d is the actual effective accelerogram duration. The maximum value $SA(f)_{\max}$ of $SA(f)$ can be taken identical to $SAHF$ because of the flatness of the spectral shape. Assuming that $a_{peak} \propto a_{rms}$ and that the spectral bandwidth of the accelerogram is nearly constant (below $f_{\max}$), we can obtain from equation 6:

$$a_{peak} \propto SAHF\left(\frac{\Delta f}{d}\right)^{0.5} \propto M_0 f_c^2 (1/d)^{0.5} \tag{7}$$

For small earthquakes, d is defined by the duration of the signal due to medium response (multi-pathing, scattering, etc.) and is magnitude dependent, thus;

$$a_{peak} \propto M_0 f_c^2 \tag{8}$$

For large earthquakes and at moderate distances, d is defined by the source process duration and thus it scales as $(1/f_c)$, so that

$$a_{peak} \propto M_0 f_c^{2.5} \tag{9}$$

Combining equation (8) and (9) we can write

$$a_{peak} \propto M_0 f_c^k \qquad \text{with } 2 \le k \le 2.5 \qquad (10)$$

From Brune's Model,

$$f_c \propto \left(\frac{\Delta\sigma}{M_0}\right)^{\frac{1}{3}}$$ and hence equation (10) takes the form

$$a_{peak} \propto M_0^{l/6} \Delta\sigma^{m/6} \quad \text{with } 1 \le l \le 2 \text{ and } 4 \le m \le 5$$

Hence at a constant M_0;

$$a_{peak} \propto \Delta\sigma^{m/6} \qquad \text{and}$$

$$k(\Delta\sigma) = \left(a_{peak} ratio\right)^n \quad \text{with } 1.5 \le n \le 1.2 \qquad (11)$$

Thus to fit the anomaly in a_{peak} by the amplification coefficient say $k(a_{peak}) = 3$, one should increase $\Delta\sigma$ by $k(\Delta\sigma)$ which accordingly to (11) varies in the range from 3.7 to 5.2. For scaling the eastern Himalayan events we use the average value of 4.5.

6. Seismic Hazard Mapping

The spatial distribution of design ground acceleration (DGA), peak ground velocity (VMAX) and peak ground displacement (DMAX) extracted from the complete synthetic seismograms computed as described in Sections 3-5 has been mapped and shown in Figures 7 to 9.

6.1 Design Ground Acceleration

The maximum values of DGA have been estimated over the north East Indian region in the epicentral zone of the great Assam earthquakes of 1897 and 1950 (Figure 7). The DGA values obtained for this region are ranging between 1.0 to 1.3 g. The Bihar-Nepal and Central Himalayan region have the DGA values between 0.3 and 0.6 g. In part of western Uttar Pradesh and in the epicentral zone of Uttarkashi earthquake of 1991 the estimated DGA values are between 0.15 to 0.3 g. In many parts of the epicentral zone of Kangra and Kutch earthquakes and in some parts of the Andaman and Nicobar islands the DGA reaches up to 0.6 g. The three metropolitan and biggest cities of India, with relevant industrial and economical importance, namely Delhi, Mumbai and Kolkata lie in the hazardous zones of the DGA map. The most severe hazard is in Delhi and its surroundings where DGA estimate is as high as

0.3 g, while in the other three big cities still DGA estimates are below 0.1 g. The DGA estimates in Peninsular India are less than 0.15 g, and only in the Latur region DGA values close to this upper limit are obtained.

6.2 Peak Velocity and Displacement

Figures 8 and 9 show the peak velocities and peak displacements mapped over the entire territory. The highest peaks are obtained in the Northeast India with velocity and displacement of 120-170 cm/sec and 60-90 cm, respectively. In the other parts of the region, like central and western Himalayas, western Uttar Pradesh, Himachal Pradesh and some parts of the Gujrat state, maximum velocity is up to 120 cm/sec and the maximum displacement to 60 cm. In the area of Andaman and Nicobar the maximum velocity and displacement are in the range 60-120 cm/sec and 30-60 cm respectively.

7. Comparison of the synthetic model against observed data

Strong Motion data have been available for the Himalayan region since 1986 from three strong-motion arrays, namely Shillong array, UP Hills array and Kangra array (Chandrasekharan and Das, 1992; Parvez *et al.*, 2001). Forty-five analogue strong motion accelerographs have been installed in Shillong array with a spacing of 10-40 km; fifty similar accelerographs are installed in Kangra array and forty in UP array with the spacing of 8 to 30 km. These arrays have recorded six earthquakes with magnitude Mw=5.2-7.2 until 1991, including the famous Uttarkashi earthquake of 1991 recorded by UP hills array and four other events by Shillong array in Northeast India. We can compare the results of our synthetic models, which are obtained from several simplifying assumptions on average input parameters, with what has been observed in the case of real earthquakes. For this comparison, we filter the observed records with a cut-off frequency of 1 Hz, the same used in the deterministic modelling. Synthetic seismograms have been computed for three large events, one from the western Himalayas (Oct., 19, 1991, Mw=6.8) and two from the eastern Himalayas (May 18, 1987, Mw=6.2; Aug. 6, 1988, Mw=7.2) and for comparison the peak acceleration (cm/sec^2) of the observed and synthetic signals at 1 Hz are plotted against the epicentral distance (km) as shown in Figure 10. As discussed in Section 5, the modified scaling law of Gusev (1983) has been used for the events of eastern Himalayas. One can see from Figure 10 that for the event of Oct. 19, 1991, our

modelling is in fairly good agreement with the observation. For the eastern Himalayan events our modelling fits well the event of Aug. 6, 1988, while the synthetic signals underestimate the peak values at the larger distances for the event of May 18, 1987. Keeping this in mind, we repeat the computation for this event using the focal depth H=75 km, as reported by Harvard catalogue and we obtain some improvement (Figure 11).

8. Discussion

A first-order deterministic evaluation of the seismic hazard of India and adjacent areas is proposed using numerically simulated ground motion. Seismic hazard maps of India and adjoining areas have also been prepared earlier by Khattri *et al.* (1984) and Bhatia *et al.* (1999) by probabilistic approach, for 10% probability of exceedance in 50 years. We compare our deterministic results with their probabilistic approach. With both the methods, the maximum hazard is estimated all along the Himalayan plate boundary, north-east India, Burmese arc and the Andaman-Nicobar islands, but there are variations in the absolute values in terms of the peak ground acceleration (g). For example Khattri *et al.* (1984) have estimated the peak values of 0.8 g in the epicentral zone of the great Assam earthquakes (eastern Himalayan) whereas Bhatia *et al.* (1999) have estimated the peak values not exceeding 0.45 g. Our results for this region give DGA values in the range from 0.6 to 1.3 g. The central and western Himalayan regions are crossed by the contour of 0.4-0.7 g according to Khattri *et al.* (1984) and 0.25-0.30 g according to Bhatia *et al.* (1999) whereas we obtain DGA values in the range 0.3 - 0.6 g. In the other high-risk zone of Andaman-Nicobar Islands 0.45 g of peak ground acceleration has been estimated by Khattri *et al.* (1984) and 0.3 g by Bhatia *et al.* (1999). For the same region our results give DGA between 0.3 and 0.6 g.

We believe that the difference between the results of Khattri *et al.* (1984) and Bhatia *et al.* (1999) is very much influenced by the choice of the attenuation relation with distance. Khattri *et al.* (1984) have used the attenuation curves of Algermissen and Perkins (1976) which are valid for the Eastern United States, whereas Bhatia *et al.* (1999) have used the attenuation relation defined by Joyner and Boore (1981) for California and the Western United States. Khattri *et al.* (1984) justify the use of the eastern US attenuation curves by comparing the Intensity attenuation curves of Indian earthquakes and found that Modified Mercally Intensity (MMI) for Indian events

attenuates like that in the Eastern US. On the other side Bhatia *et al.* (1999) do not give any reason for the use of the western United States attenuation law in their study. In the recent study of Parvez *et al.* (2001), the attenuation curves of several parts of the world have been compared with those they obtained for the Indian region. They have found that the attenuation of peak accelerations with distance in the western US is in agreement with that in the western Himalayan region, whereas for the eastern Himalayas the level is three times higher. In terms of shape of attenuation curves and the decay of acceleration, the eastern US attenuation curves represents the best analogy with eastern Himalayas. This evidence makes it clear why Bhatia *et al.* (1999) underestimates the values for the eastern Himalayan region while Khattri *et al.* (1984) slightly overestimates the values for the western and central Himalayas.

We have checked the depth dependency while comparing the event of May 18, 1987, with our computations, and we got a better fit at large distances assuming the hypocentral depth of 75 km (Figure 11). This clearly indicates that the deterministic modelling is a strong and powerful tool which is able to predict the ground motion in a very close agreement with the observed data, if it is provided sufficiently precise and accurate information on structural model, focal mechanism and earthquake magnitude. If such data are not available, it is easy enough to run a parametric analysis and to produce several deterministic scenarios that can be compared and evaluated in order to understand better the influence of each input parameter on the ground shacking distribution.

Even after using generalized assumptions and average properties of the input parameters, our results compare well with the peak ground acceleration observed during the Uttarkashi event of Oct. 6, 1991 and are also well in agreement with the Aug. 6, 1988 of the eastern Himalayas (the region of unusual high peak acceleration). On January 26, 2001, while the nation was celebrating the Republic Day, a large earthquake of magnitude Mw=7.6 occurred in western India near Bhuj. It was undoubtedly the worst earthquake to have hit Independent India. More than twenty thousands people are reported to be dead and hundreds of thousands were injured with an estimated economic loss of over 5 billions of US $. This was shocking news that generated untold misery and captured media attention around the world. This event has given us an opportunity to further check our deterministic prediction of ground motion. We performed a new computation using the preliminary source parameters of this event (Ms=7.9, Strike=292, Dip=36, Slip=136, Depth=15 km.). The idea was to

see how well our prediction fits with the observed scenario. We ended up with only 4 cells out of about 500 where the DGA values determined including the Bhuj event exceed the values given in Figure 7 in such a way that an increment of at most 1 degree in intensity could be expected (Shteinberg et al., 1993; Panza et al., 1997). Therefore it comes out that the groundshacking scenario due to the Bhuj event does not add much to the foreseen scenario.

The first order zoning of the Indian subcontinent we have obtained, can be considered a good starting point for more detailed studies that should be carried out in areas of specific interest. Such studies require a better knowledge of the source characteristics and of the structural properties, mostly of the upper sedimentary layers, in order to estimate the site effects for several scenario earthquakes. In this context, we are now working on the seismic microzonation of Delhi City, the capital of India, as it comes in a zone with maximum DGA value up to 0.3 g.

8. Conclusion

The deterministic seismic hazard maps in terms of DMAX, VMAX, and DGA have been prepared for the Indian territory and adjacent areas by computing realistic synthetic seismograms. Generally, the seismic hazard is mainly controlled by the strongest event in the area and it is found to be highest in eastern Himalayan and Burmese arc region, where the design ground acceleration (DGA) exceeds 1 g. In the other regions prone to strong events, like Bihar-Nepal, Kangra, Kutch and Andaman and Nicobar islands, DGA values as high as 0.6 g have been obtained. The peak velocity and displacement are also high in the same hazardous zones. The observed peak ground acceleration due to one event in western Himalayas and two events in eastern Himalayas has been found in good agreement with our modelling.

The deterministic modelling of hazard for the Indian territory yields meaningful results validated by recent observations made in connection with events occurred after 1998, the upper limit of the catalogue we used. It provide us with a powerful and economically valid scientific tool for seismic zonation and hazard assessment. The main advantage of the method lies in its ability to directly estimate the effects of source mechanics and wave propagation, while local site effects are roughly considered when using the design spectra to obtain the DGA from the synthetic response spectra. We believe that the data we present here will contribute to a better understanding of the seismic hazard in India and neighbouring areas.

Furthermore, our multidisciplinary approach may help to those earthquake and civil engineers who wish to undertake comprehensive and detailed studies of earthquake hazard especially in Himalayan eastern region, eastern and western India and some big cities like Delhi, Mumbai and Kolkata.

Acknowledgments

We thank the Department of Science and Technology (DST), Govt. of India for providing the strong motion data. We are very thankful and grateful to Prof. A.A. Gusev for his constructive suggestion in scaling the events of eastern Himalayas. One of us (IAP) is thankful to Prof. G. Furlan, Head, Training and Research in Italian Laboratory (TRIL) program of ICTP for providing the grant to stay at the Department of Earth Sciences of Trieste University. The financial support from the IUGS-UNESCO-IGCP project 414 "Realistic Modelling of Seismic Input for Megacities and large Urban Areas" is also thankfully acknowledged.

References

Aki, K., 1987. Strong motion seismology. *In: Erdik, M. and Toksoz, M. (eds.), Strong Ground Motion Seismology, NATO ASI Series C, Mathematical and Physical Science,* D. Reidel Publishing Company, Dordrecht, vol. **204**, pp. 3-39.

Algermissen, S.T. & Perkins, D.M., 1976. A probabilistic estimate of maximum acceleration in rock in the contiguous United States, *U.S. Geol. Surv. Open-file Rep.,* 76-416, 45 pp.

Alvarez, L., Vaccari, F. & Panza, G.F., 1999. Deterministic seismic zoning of eastern Cuba, *Pure & Appl. Geophys.*, **156**, 469-486.

Aoudia, A., Vaccari, F., Suhadolc, P. & Meghraoui, M., 2000. Seismogenic potential and earthquake hazard assessment in the Tell Atlas of Algeria, *J. Seismology*, **4**, 79-98.

Auden, J.B., 1959. Earthquakes in relation to the Damodar Valley Project, *Proc. Symp. Earthquake Eng., 1st University of Roorkee, Roorkee.*

Bhatia, S.C., Kumar, R. & Gupta, H. K., 1999. A probabilistic seismic hazard map of India and adjoining regions, *Annali di Geofisica,* **42**, 1153-1164.

Bourjot, L., & Romanowicz, B., 1992. Crust and upper mantle tomography in Tibet using surface waves, *Geophys. Res. Letters,* **19**, 881-884.

Bus, Z., Szeidovitz, G. & Vaccari, F., 2000. Synthetic seismograms based deterministic seismic zoning for the Hungarian Part of the Pannonian Basin, *Pure & Appl. Geophys.*, **157**, 205-220.

Chandra, U., 1977. Earthquakes of Peninsular India-A seismotectonic study, *Bull. Seism. Soc. Am.,* **67**, 1387-1413.

Chandra, U., 1978. Seismicity, earthquake mechanics and tectonics along the Himalayan mountain range and vicinity, *Phys. Earth Planet. Inter.,* **16**, 109-131.

Chandrasekaran, A.R. & Das, J.D., 1992. Strong Motion arrays in India and analysis of data from Shillong array, *Current Science*, **62**, 233-250.

Costa, G., Panza, G.F., Suhadolc, P. & Vaccari, F., 1993. Zoning of the Italian territory in terms of expected peak ground acceleration derived from complete synthetic seismograms, in: *R. Cassinis, K. Helbig and G.F. Panza (eds.), Geophysical Exploration in Areas of Complex Geology, II, J. Appl. Geophys.* **30**, 149-160.

Cotte, N., Pedersen, H., Campillo, M., Mars, J., Ni, J.F., Kind, R., Sandvol, E. & Zhao, W., 1999. Determination of the crustal structure in southern Tibet by displacement and amplitude analysis of Rayleigh waves, *Geophys. J. Int.,* **138**, 809-819.

Curtis, A. & Woodhouse, J.H., 1997. Crust and upper mantle shear velocity structure beneath the Tibetan plateau and surrounding regions from interevent surface wave phase velocity inversion, *J. Geophys. Res.*, **102**, 11,789-11,813.

Deshikachar, S.V., 1974. A review of the tectonic and geological history of eastern India in terms of "plate tectonics" theory, *J. Geol. Soc. India*, **15**, 137-149.

El-Sayed, A., Vaccari, F. & Panza, G.F., 2001. Deterministic seismic hazard in Egypt, *Geophys. J. Int.*, **144**, 555-567.

Eremenko, N.A. & Negi, B.S., 1968. A guide to the tectonic map of India. *Oil and Natural Gas Commission, India,* pp 1-15.

Fitch, T.J., 1970. Earthquake mechanism in the Himalayan, Burmese and Andaman regions and the continental tectonics in Central Asia, *J. Geophys. Res.*, **75**, 2699-2709.

Florsch, N., Faeh, D., Suhadolc, P. & Panza, G.F., 1991. Complete synthetic seismograms for high frequency multimodal SH waves. *Pure & Appl. Geophys.*, **136**, 59-560.

Gansser, A., 1964. Geology of the Himalayas, *Interscience, New York.* 289 pp.

Gansser, A., 1977. The great suture zone between Himalaya and Tibet: A preliminary account, Himalaya: *Science de la Terre, edited by C. Jest, Colloq. Int. C.N.R.S.*, **268**, 181-192.

Gaur, V.K. & Chouhan, R.K.S., 1968. Quantitative measures of seismicity applied to Indian regions. *Bull. Indian Soc. Earthquake Technol.*, **5**, 63-78.

Guha, S.K., 1962. Seismic regionalization of India, *Proc. Symp. Earthquake Eng., 2nd, Roorkee,* pp. 191-207.

Gusev, A.A., 1983. Descriptive statistical model of earthquake source radiation and its application to an estimation of short period strong motion, *Geophys. J.R. astr. Soc.*, **74**, 787-808.

Joyner, W.B. & Boore, D.M., 1981. Peak horizontal acceleration and velocity from strong-motion records including records from the 1979 Imperial Valley, California, Earthquake, *Bull. Seism. Soc. Am.*, **71**, 2011-2038.

Kaila, K.L. & Rao, M., 1979. Seismic zoning maps of Indian subcontinent. *Geophys. Res. Bull.*, **17**, 293-301.

Kanamori, H., 1977. The energy release in great earthquakes, *J. Geophys. Res.*, **82**, 2981-2987.

Khattri, K.N., Rogers, A.M., Perkins, D.M. & Algermissen, S.T., 1984. A seismic hazard map of India and adjacent areas, *Tectonophysics,* **108**, 93-134.

Khatrri, K.N., 1987. Great earthquakes, seismicity gaps and potential for earthquake disaster along the Himalaya plate boundary, *Tectonophysics*, **138**, 79-92.

Krishnan, M.S., 1968. Geology of India and Burma, *Higginbothams, Madras,* 536 pp.

Lyon-Caen, H., 1986. Comparison of the upper mantle shear wave velocity structure of the Indian shield and the Tibetan plateau and tectonics implications, *Geophys. J.R. astr. Soc.*, **86**, 727-749.

Markusic, S., Suhadolc, P., Herak, M. & Vaccari, F., 2000. A contribution to seismic hazard in croatia from deterministic modelling, *Pure & Appl. Geophys.*, **157**, 185-204.

Mitchell, B., Yu Pan, Jiakang Xie & Lianli Cong, 1997. Lg coda Q variation across Eurasia and its relation to crustal evolution. *J. Geophys. Res.*, 102, 10, 767-22,779.

Mithal, R.S. & Srivastava, L.S., 1959. Geotectonic position and earthquakes of Ganga-Brahmputra region. *Proc. Symp. Earthquake Eng., 1st Univ. Roorkee, Roorkee.*

Mohan, G. & Rai, S.S., 1995. Large-scale three-dimensional seismic tomography of the Zagros and Pamir-Hindukush region, *Tectonophysics*, **242**, 255-265.

Mohan, G., Rai, S.S. & Panza, G.F., 1997. Shear velocity structure of the laterally heterogeneous crust and uppermost mantle beneath the Indian region, *Tectonophysics*, **277**, 259-270.

Molchan, G., Kronrod, T. & Panza, G.F., 1997. Multi-scale seismicity model for seismic risk, *Bull. Seism. Soc. Am.*, **87**, 1220-1229.

Molnar, P., Fitch, T.J. & Wu-Francis, T., 1973. Fault plane solutions of shallow earthquakes and contemporary tectonics in Asia, *Earth & Planet. Sci. Let.*, **19**, 101-112.

Naqvi, S.M. & Rogers, J.J.W., 1987. Precambrian Geology of India, *(Oxford Monogr. Geol. Geophys., 6)* Oxford University Press, Oxford, 223.

Oldham, R.D., 1899. Report on the great earthquake of June 12, 1897, *Mem. Geol. Surv. India,* **29**, 1-379.

Orozova-Stanishkova, I.M., Costa, G., Vaccari, F. & Suhadolc, P., 1996. Estimation of 1 Hz maximum acceleration in Bulgaria for seismic risk reduction purposes, *Tectonophysics*, **258**, 263-274.

Panza, G.F., 1985. Synthetic seismograms: The Rayleigh waves model summation, *J. Geophys.*, **58**, 125-145.

Panza, G. F. & Suhadolc, P., 1987. Complete strong motion synthetics. In: B. A. Bolt (ed.) Seismic Strong Motion Synthetics, Computational Techniques 4, Academic Press, Orlando, 153-204.

Panza, G.F., Vaccari, F., Costa, G., Suhadolc, P. & Faeh, D., 1996. Seismic input modelling for zoning and microzoning, *Earthquake Spectra*, **12**, 529-566.

Panza, G.F., Cazzaro, R. & Vaccari, F., 1997. Correlation between macroseismic intensities and and seismic ground motion parameters, *Annali di Geofisica*, **40**, 1371-1382.

Panza, G.F., Vaccari, F. & Romanelli, F., 1999. Deterministic seismic hazard assessment. *F. Wenzel et al., (eds.), Vrancea Earthquakes. Tectonic and Risk Mitigation,* Kluwer Academic Publishers, The Netherland, 269-286.

Panza, G.F., Romanelli, F. & Vaccari, F., 2001. Seismic wave propagation in laterally heterogeneous anelastic media: theory and application to seismic zonation. *R. Dmowska and B. Saltzman (eds), Advances in Geophysics*, Academic Press, San Diego, USA, **43**, 1-95.

Parvez, I.A. & Ram, A., 1997. Probabilistic assessment of earthquake hazards in the north-east Indian Peninsula and Hidukush region, *Pure & Appl. Geophys.*, **149**, 731-746.

Parvez, I.A. & Ram, A., 1999. Probabilistic assessment of earthquake hazards in the Indian Subcontinent, *Pure & Appl. Geophys.*, **154**, 23-40.

Parvez, I.A., Gusev, A.A., Panza, G.F. & Petukhin, A.G., 2001. Preliminary determination of the interdependence among strong motion amplitude, earthquake magnitude and hypocentral distance for the Himalayan region, *Geophys. J. Int.*, **144**, 577-596.

Prakasam, K.S. & Rai, S.S., 1998. Teleseismic delay-time tomography of the upper mantle beneath southeastern India: imprint of Indo-Antarctica rifting, *Geophys. J. Int.*, **133**, 20-30.

Radulian, M., Vaccari, F., Mândrescu, N., Panza, G.F. & Moloveanu, C.L., 2000. Seismic hazard of Romania: Deterministic approach, *Pure & Appl. Geophys.*, **157**, 221-247.

Ram, A. & Mereu, R.F., 1977. Lateral variations in upper mantle structure around India as obtained from Gauribidanur seismic array data, *Geophys. J.R. astr. Soc.*, **49**, 87-113.

Ramesh, D.S., Srinagesh, D., Rai, S.S., Prakasam, K.S. & Gaur, V.K., 1993. High-velocity anamoly under the Deccan Volcanic Province, *Phys. Earth Planet. Inter.*, **77**, 285-296.

Roecker, S.W., 1982. Velocity structure of the Pamir Hindukush region: Possible evidence of subducted crust, *J. Geophys. Res.*, **87**, 945-959.

Shanker, D. & Sharma, M.L., 1998. Estimation of seismic hazard parameters for the Himalayas and its vicinity from complete data files, *Pure & Appl. Geophys.*, **152**, 267-279.

Shteinberg, V., Saks, M., Aptikaev, F., Alkaz, V., Gusev, A., Erokhin, L., Zagradnik, I., Kendzera, A., Kogan, L., Lutikov, A., Popova, E., Rautian, T. & Chernov, Yu., 1993. Methods of seismic ground motions estimation (Handbook). Seismic ground motion prediction. *Engineering seismology problems*, Issue 34. Moscow, Nauka, 5-94. (in Russian)

Singh, D.D., 1987. Crust and upper mantle velocity structure beneath the north and central India from the phase and group velocity of Rayleigh and Love waves, *Tectonophysics,* **139**, 187-203.

Singh, D.D., 1988. Crust and upper mantle velocity structure beneath the northern and central Indian ocean from the phase and group velocity of Rayleigh and Love waves, *Phys. Earth Planet. Inter.*, **50**, 230-239.

Singh, D.D., 1991. Anelasticity of the crust and upper mantle beneath north and central India from the inversion of observed Love and Rayleigh wave attenuation data, *Pure & Appl. Geophys.*, **135**, 545-558.

Singh, D.D., 1994. Shear wave velocity over the eastern Indian subcontinent., *Tectonophysics,* 230, 127-134.

Srinagesh, D. & Rai, S.S., 1996. Teleseismic tomographic evidence for contrasting crust and upper mantles in south Indian Archaen terrains, *Phys. Earth Planet. Inter.*, **97**, 27-41.

Tondon, A.N., 1956. Zones of India liable to earthquake damage. *Ind. J. Meteorol. Geophys.*, **10**, 137-146.

Vaccari, F., 1995. LP-displacement hazard evaluation in Italy. *In: Proc. 24th General Assembly of the European Seismological Commission, Athens,* **3**, 1489-1498.

Valdiya, K.S., 1973. Tectonic framework of India: a review and interpretation of recent structural and tectonic studies. *Geophys. Res. Bull.,* **11**, 79-114.

Verma, R.K., 1991. Geodynamics of the Indian Peninsula and the Indian Plate Margin, *Oxford and IBH Publishing Co, Pvt. Ltd., New Delhi,* pp. 278-321.

Wadia, D. N., 1975. Geology of India, *Tata McGraw Hill, New Delhi,* 508 pp.

Yu, G., Khattri, K.N., Anderson, J.G., Brune, J.N., Zeng, Y., 1995. Strong ground motion from the Uttarkashi, Himalaya, India, earthquake: Comparison of observations with synthetics using the composite source model, *Bull. Seism. Soc. Am.*, **85**, 31-50.

Zivcic, P., Suhadolc, P. & Vaccari, F., 2000. Seismic zonation of Slovenia based on deterministic hazard computation, *Pure & Appl. Geophys.*, **157**, 171-184.

Table 1: Catalogue completeness for the Indian Subcontinent (after Khattri, 1987)

Time	Magnitude
1800-1900	M>=8.0
1901-1925	M=7.0
1926-1950	M=6.5
1951-1960	M=6.0
1961-1982	M=5.0

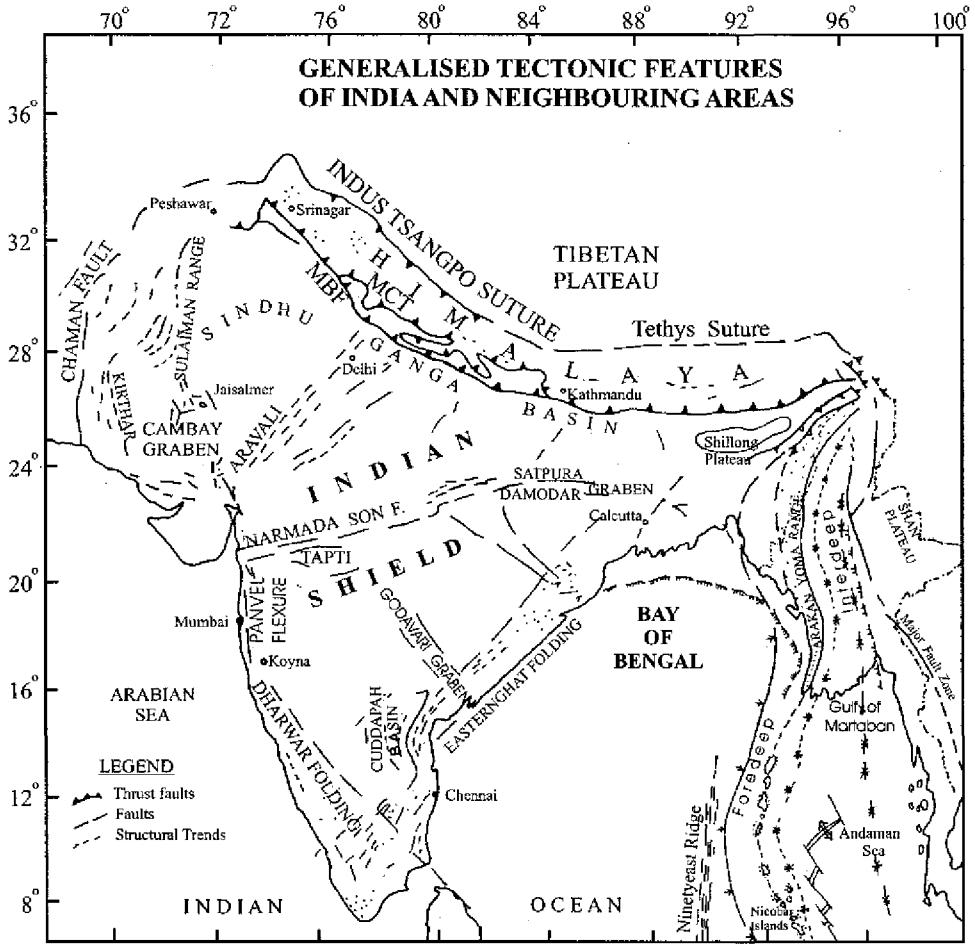

Figure 1. Generalised tectonic map of India and adjacent areas (modified after Khattri *et al.*, 1984 and Parvez and Ram, 1999)

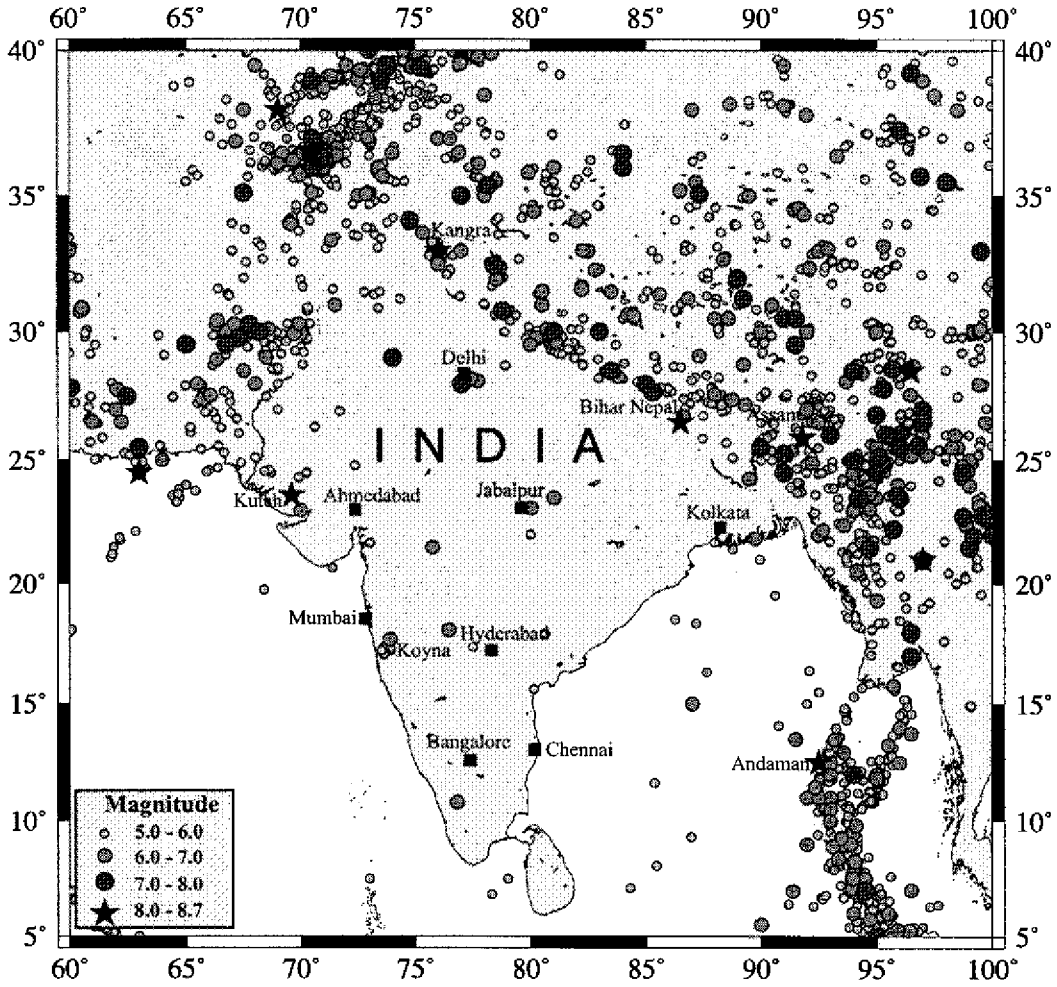

Figure 2. Seismicity map of the Indian Subcontinent. The used space distribution of earthquakes for the period 1819 to 1998.

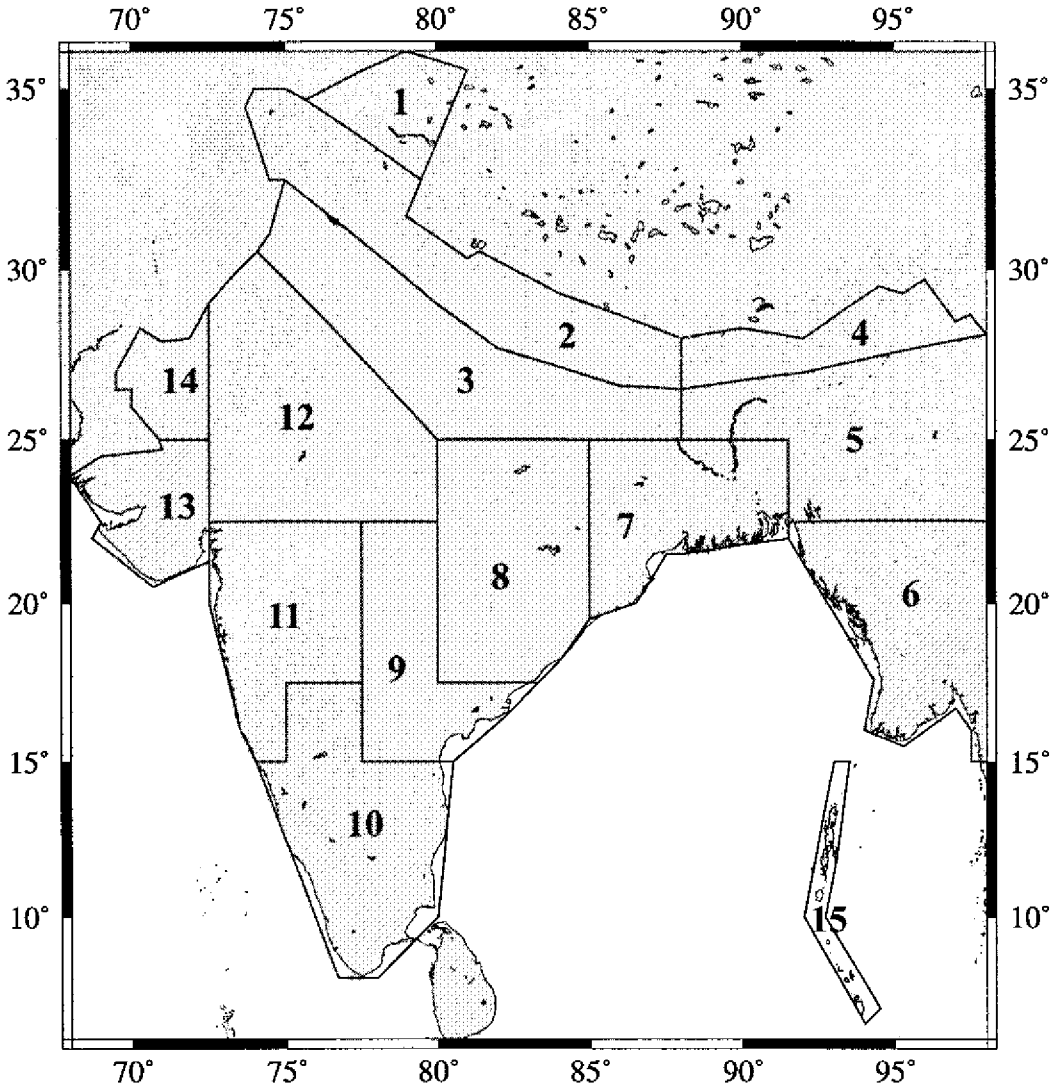

Figure 3. Boundaries of regional structural polygons. The numbers of each polygon correspond with those given in Figure 4.

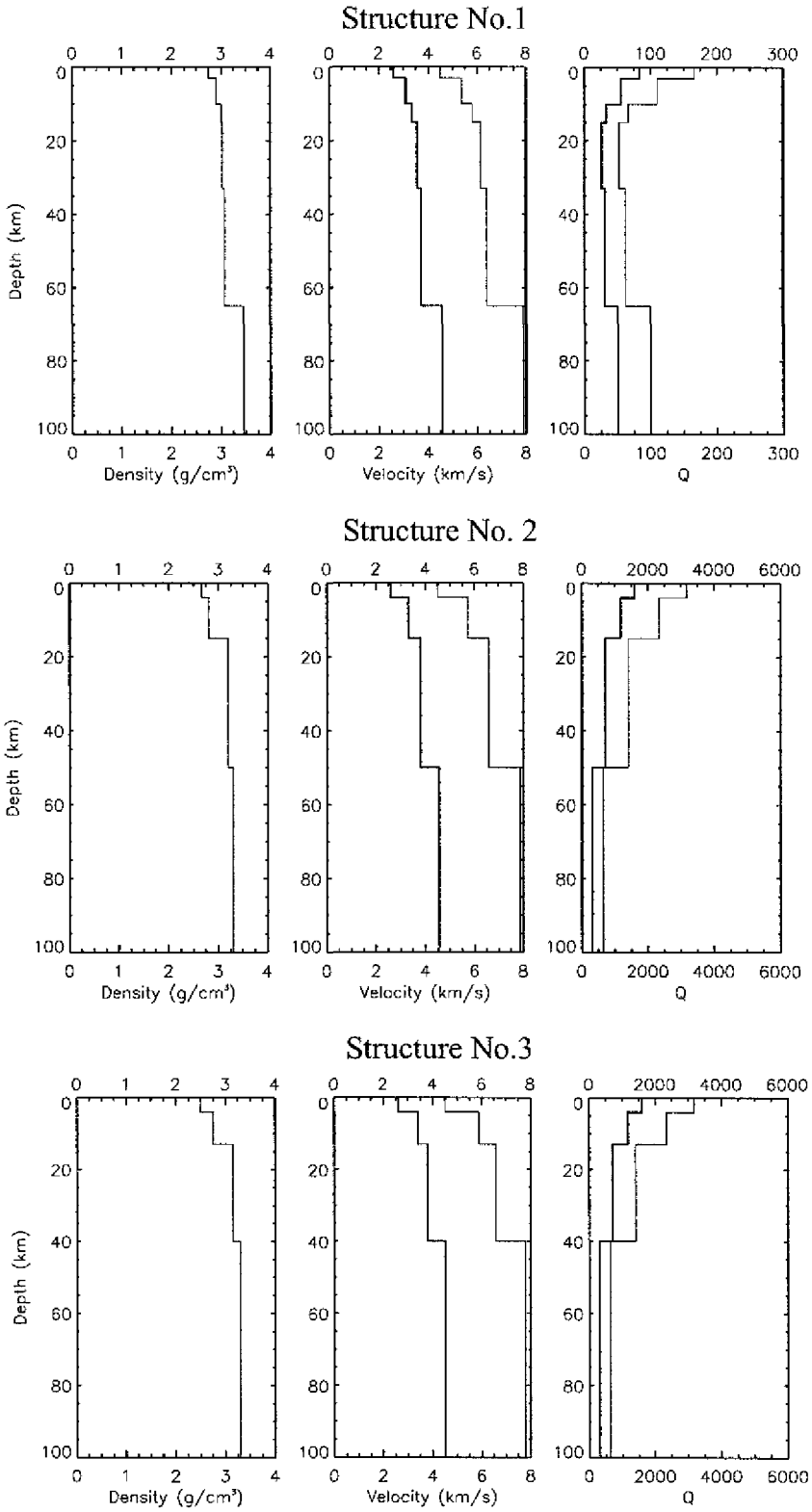

Figure 4. Average lithospheric structures for the regional structural polygons shown in Figure 3. Density in g/cm^3, P- and S-wave velocities in km/sec, and the corresponding quality factor (thick line for S-waves and thin for P-waves) are shown for the first 100 km of depth.

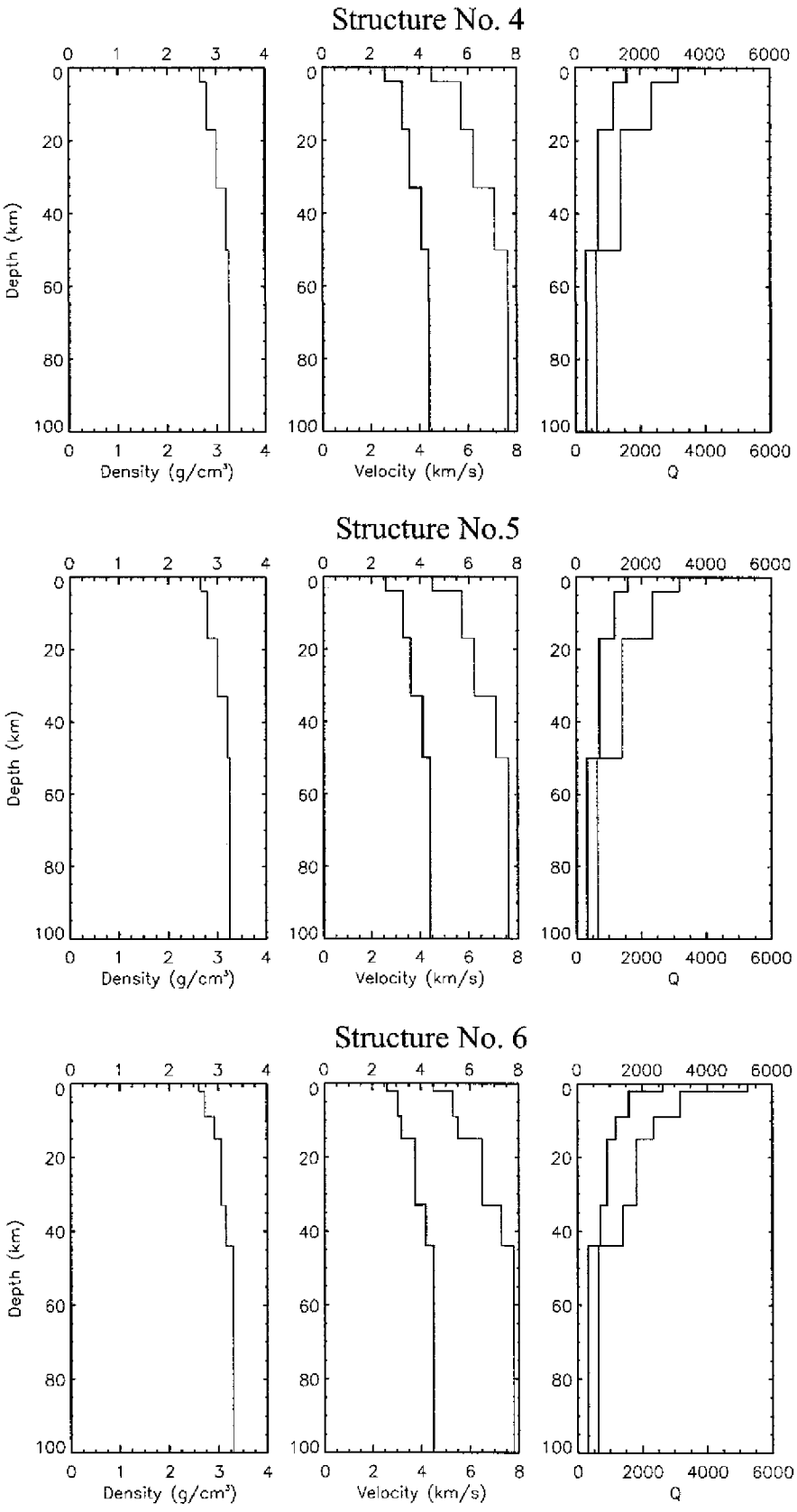

Figure 4. (continued)

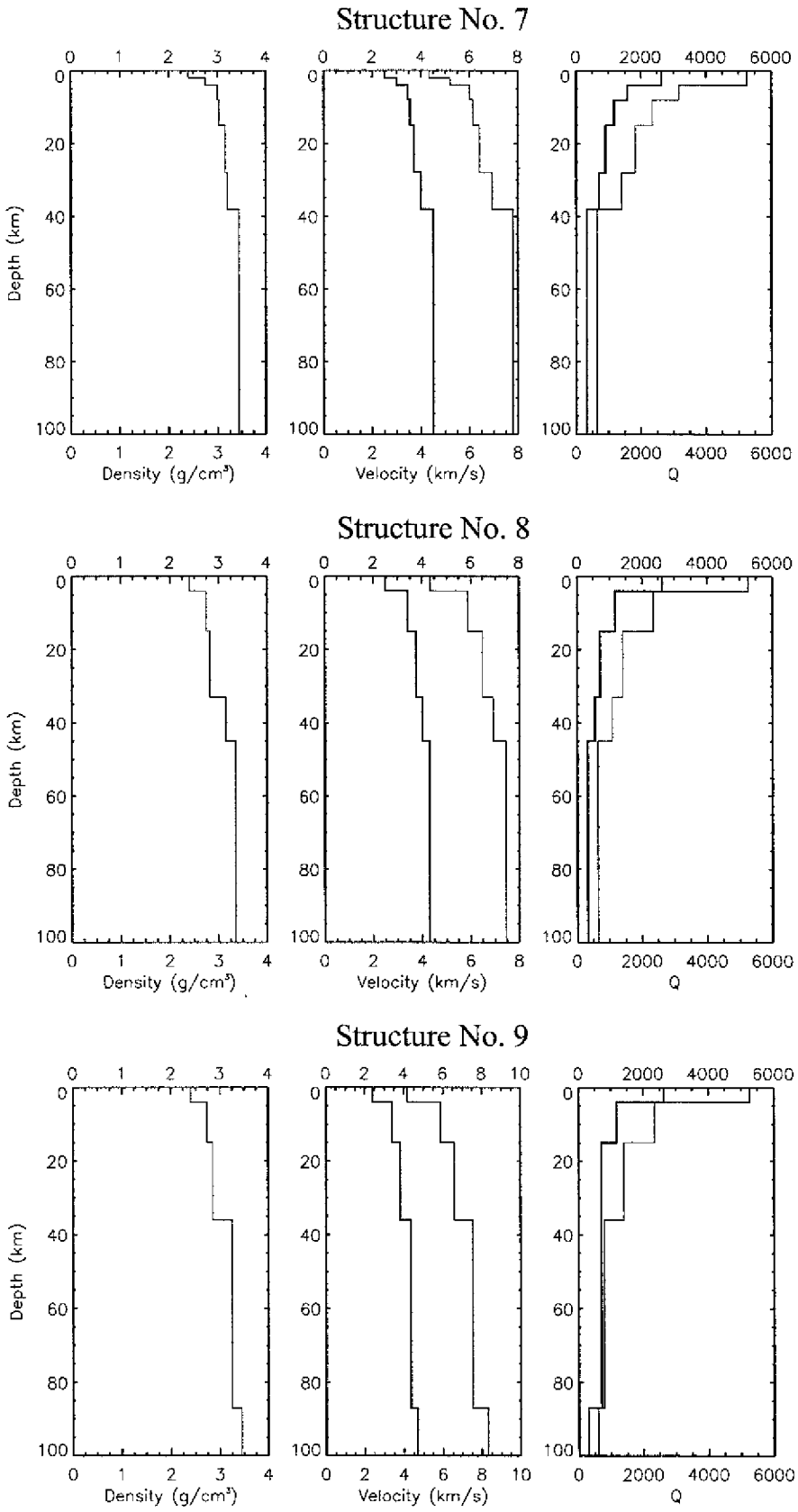

Figure 4. (continued)

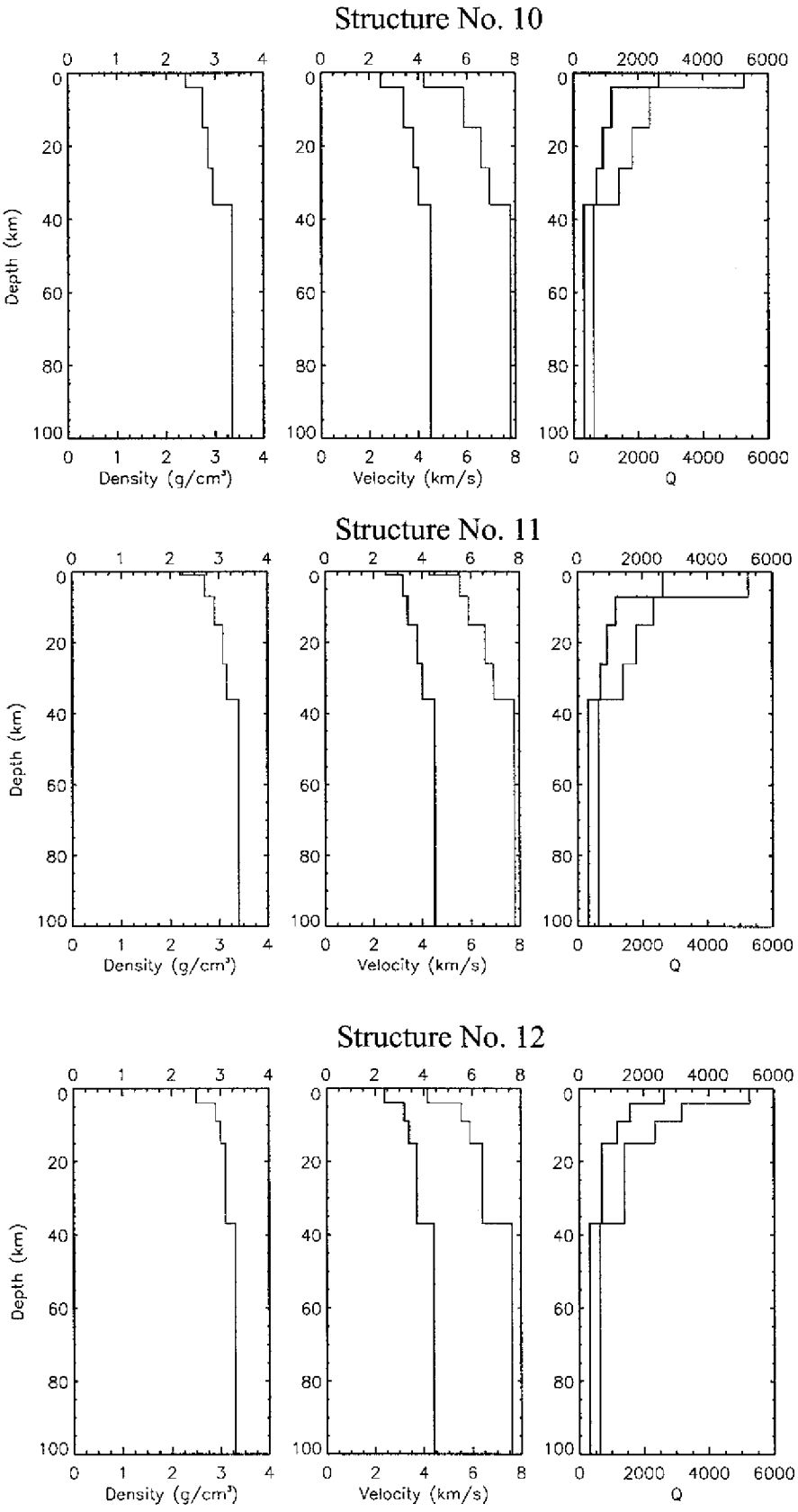

Figure 4. (continued)

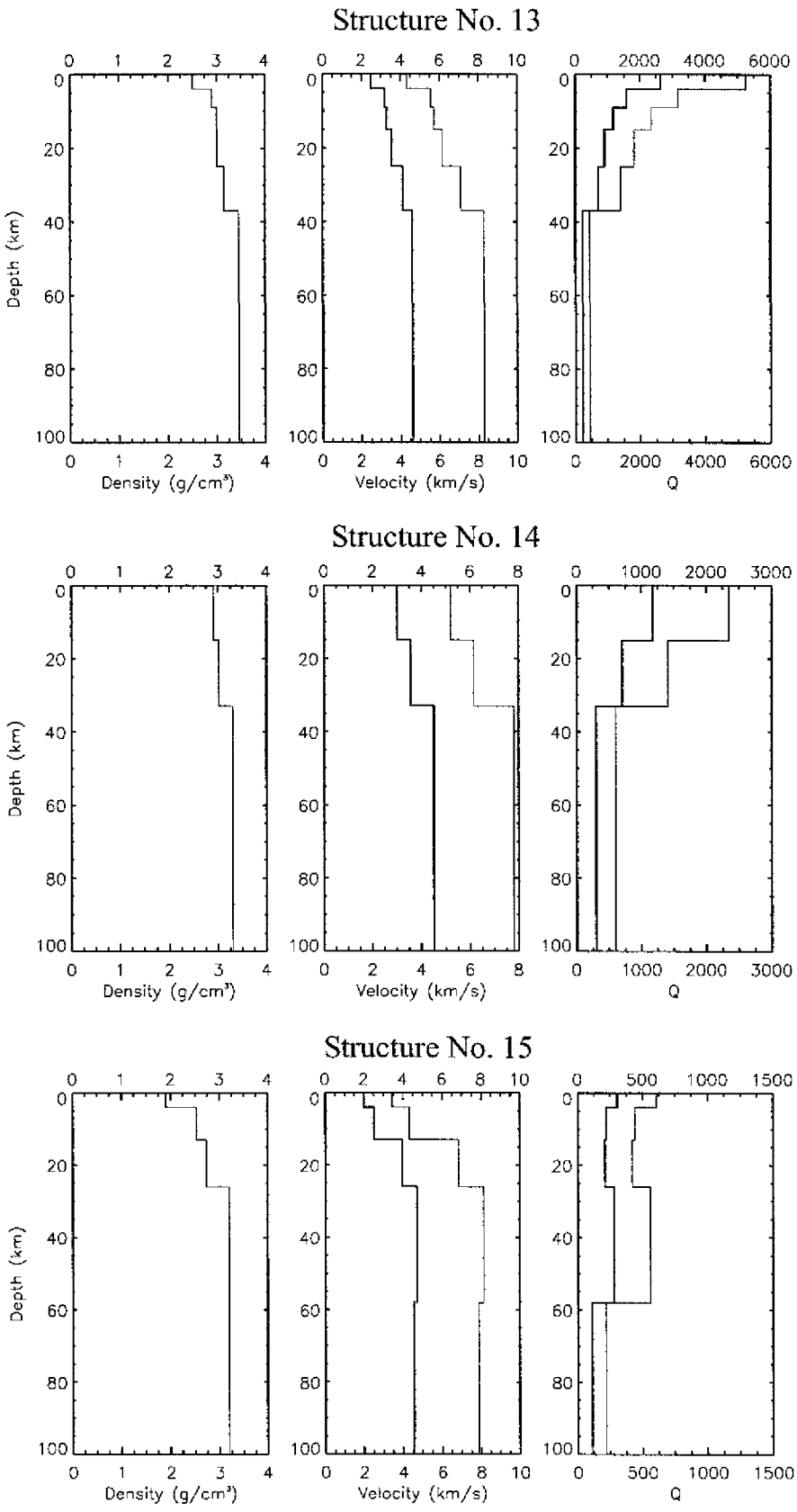

Figure 4. (continued)

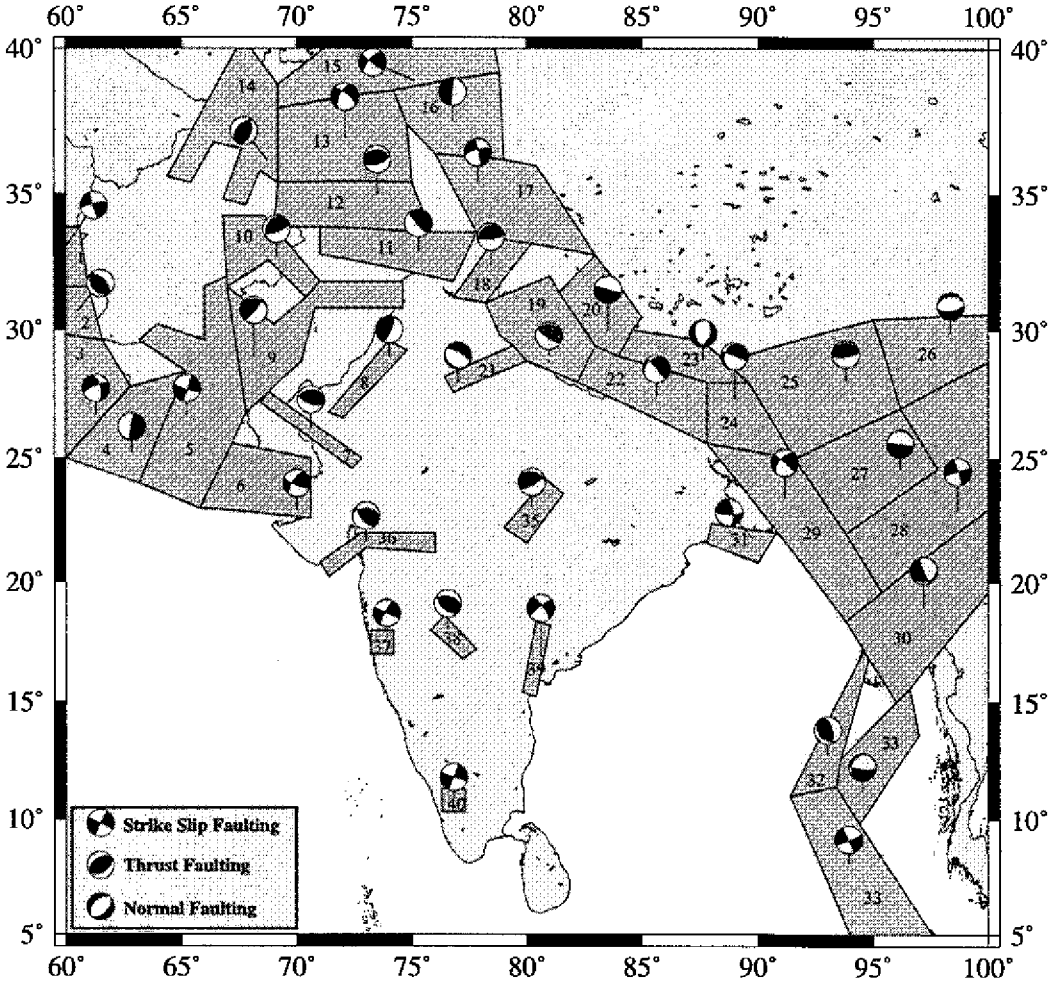

Figure 5. Boundaries of the seismogenic zones. For each seismogenic zone the assigned fault plane solution is shown.

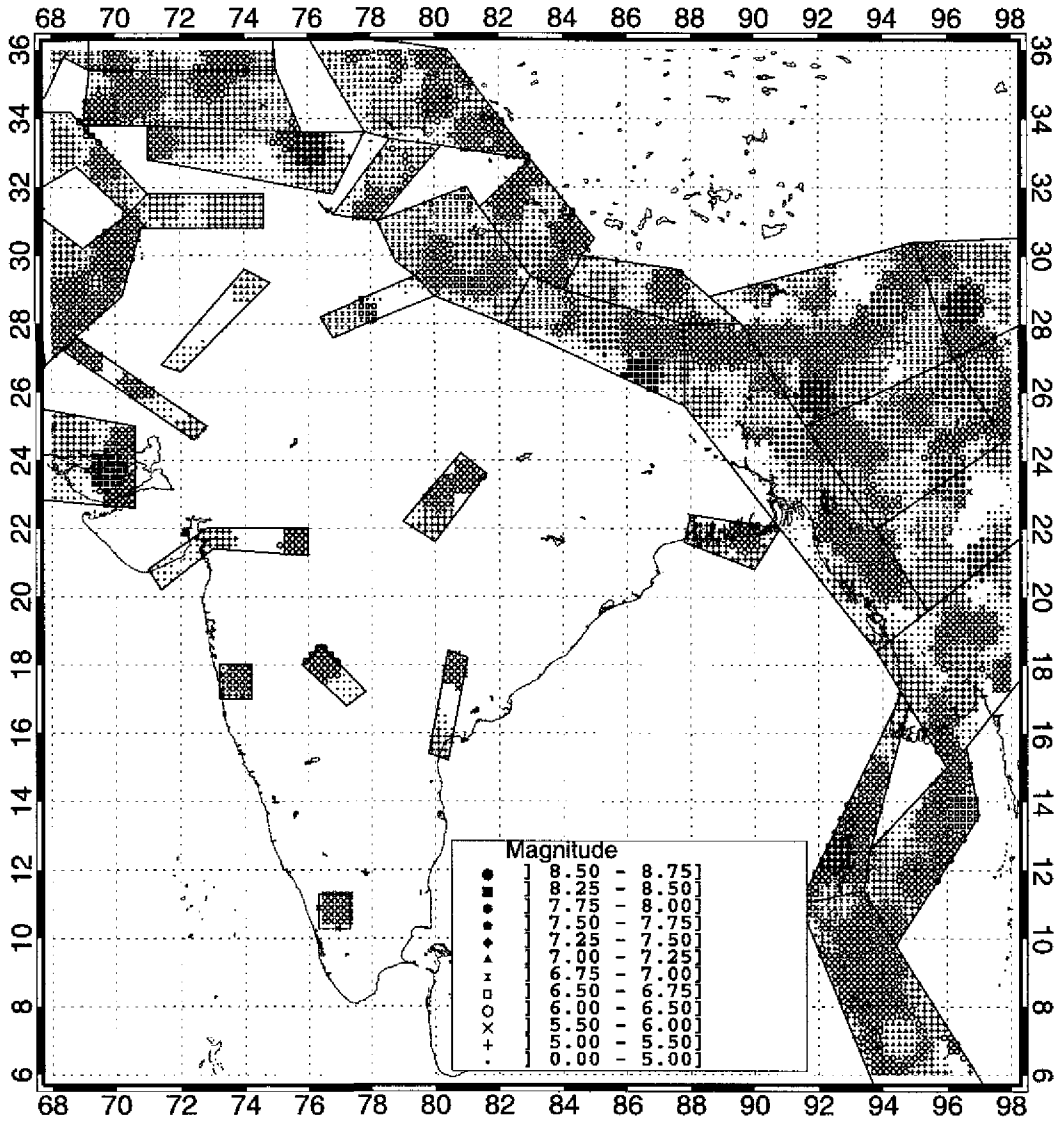

Figure 6. Representation of the "smoothed" seismicity within each seismogenic zone.

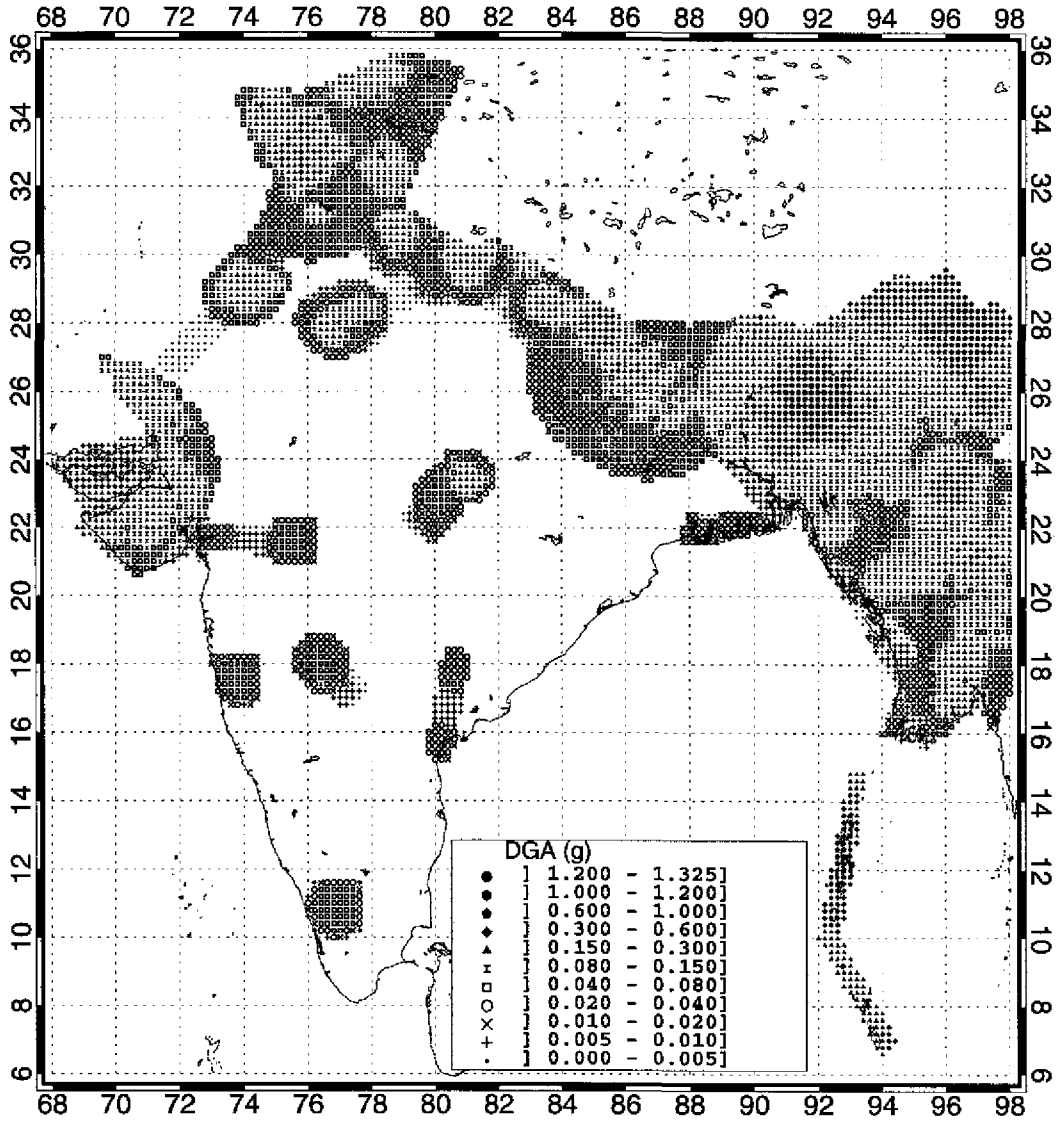

Figure 7. Spatial distribution of the design ground acceleration (DGA) in g.

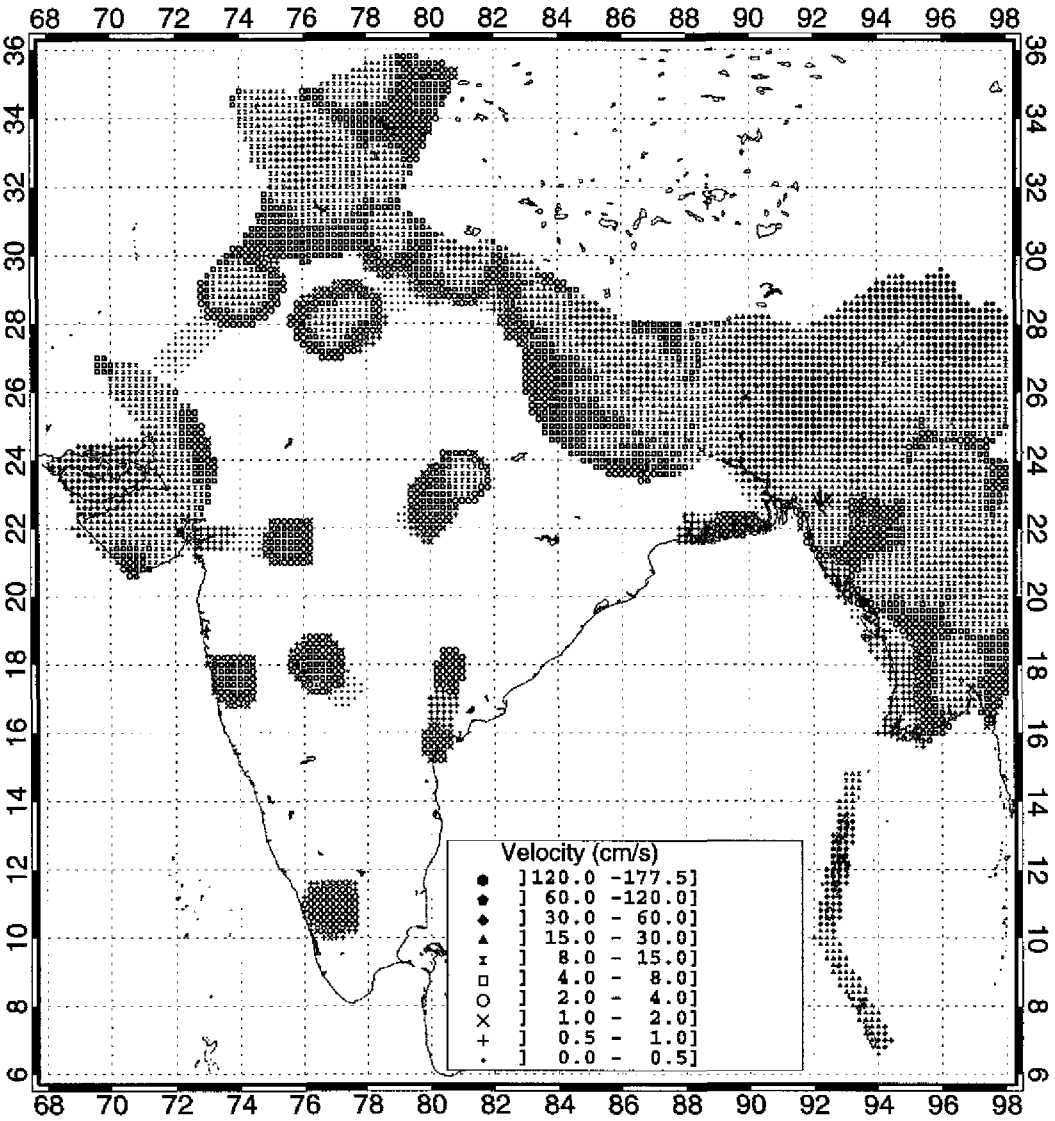

Figure 8. Same as figure 8 for peak ground velocity in cm/sec.

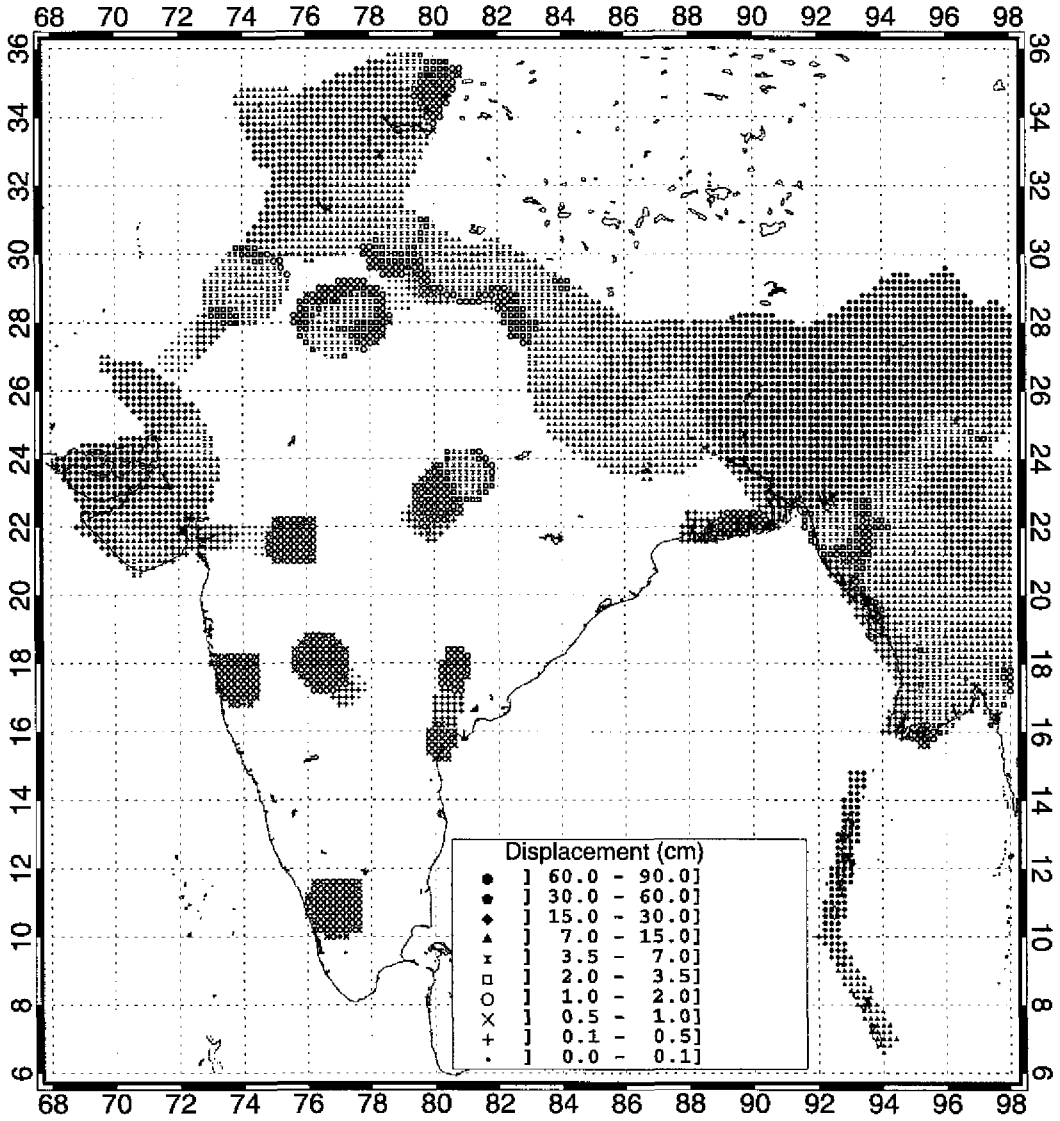

Figure 9. Spatial distribution of the estimated peak ground displacement in cm.

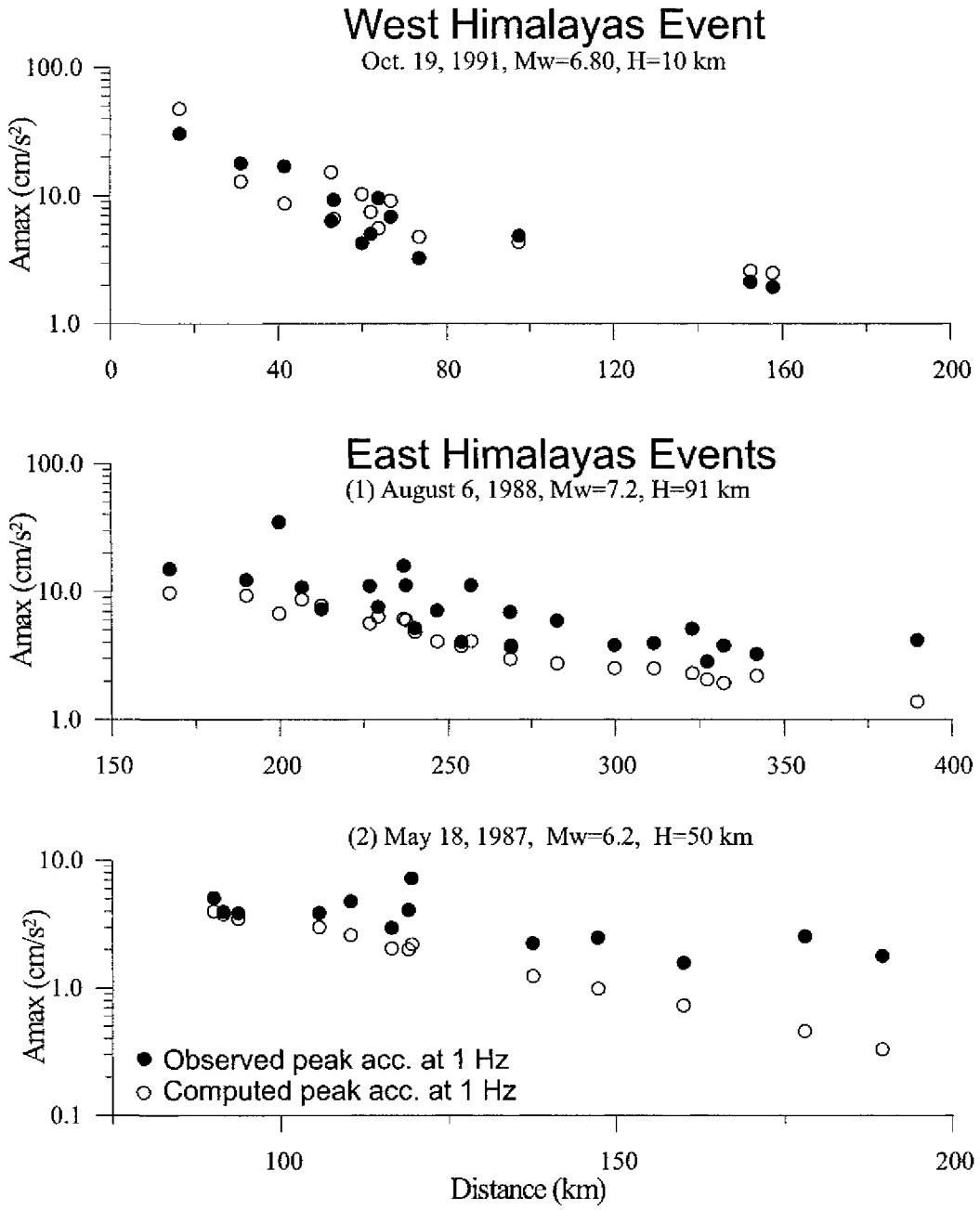

Figure 10. Comparison of observed and synthetic peak acceleration at 1 Hz with distance for the events of western and eastern Himalayas. The moment magnitude (Mw) and NEIC focal depth (H) is also indicated.

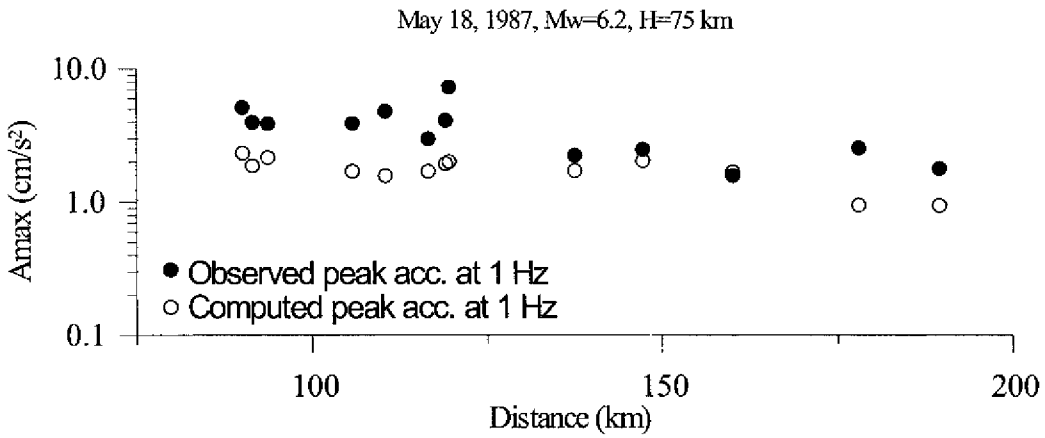

Figure 11. Same as Figure 10 for the event of May 18, 1987 at H=75 km (CMT) for the other events NEIC and CMT depths are similar.